Synthesis and Characterization of Oligomers Containing the α-Aminoalkylphenone Chromophore as Oligomeric Photoinitiator

Guodong Ye,[1,2] Hua Zhou,[3] Jianwen Yang,[1] Zhaohua Zeng,[1] Yonglie Chen[1]

[1]*School of Chemistry and Chemical Engineering, Sun Yat-Sen University, Guangzhou 510275, People's Republic of China*
[2]*Department of Chemistry, Guangzhou Medical College, Guangzhou 510182, People's Republic of China*
[3]*Obstetrics and Gynecology Research Institute of the No. 2 Municipal People's Hospital of Guangzhou Medical College, Guangzhou 510150, People's Republic of China*

Received 8 December 2004; accepted 19 May 2005
DOI 10.1002/app.22956
Published online 19 January 2006 in Wiley InterScience (www.interscience.wiley.com).

ABSTRACT: An oligomeric photoinitiator containing α-aminoalkylphenone photoactive chromophore in the main chain was prepared from diphenyl ether, α-chloroisobutyryl chloride, and piperazine through acylation, bromination, epoxidation, and polycondensation. The obtained oligomeric photoinitiator was characterized by GPC, TGA, traditional DSC, FTIR, NMR, UV–vis absorption, and fluorescence spectroscopy. The number-average molecular weight (M_n) of the oligomeric photoinitiator was determined to be 2000–4000. The excitation and emission wavelengths of the fluorescence spectra were 376 and 473 nm, respectively. The thermal stability of the oligomer was found to be perfect with a decomposition temperature greater than 300°C. All the spectroscopic and thermal analyses clearly confirmed the consistence of property and structure. In a comparative photo-DSC investigation, the oligomeric photoinitiator showed high photoinitiating efficiency while using 1,6-hexanediol diacrylate as monomer. © 2006 Wiley Periodicals, Inc. J Appl Polym Sci 99: 3417–3424, 2006

Key words: oligomers; polycondensation; photopolymerization; coatings

INTRODUCTION

UV curing has found an increasing number of industrial applications over the past few decades and will find even more areas of application in the years to come. In UV curing the unsaturated bonds cleave, and the monomers start a rapid photopolymerization with the aid of a photoinitiator when the uncured mixture is exposed to high-energy UV light. Hence, the photoinitiator plays a crucial role in UV-curable formulations.[1]

Some photoinitiators are sensitive enough to light. One of the main features of a photoinitiator is the weak bond in its structure. The weak bond breaks up while exposed to irradiation, and active free radicals are produced. Compounds used for this reaction are known as type I photoinitiators, and the homolytic cleavage usually occurs between the carbonyl group and an adjacent α-carbon (α-cleavage). Other photoinitiators undergo a mechanism called hydrogen abstraction; these are classified as type II photoinitiators.[2] Despite the difference between these two triggering mechanisms, the practical result is to initiate polymerization upon phototriggering.

Many commercial photoinitiators already have been developed in this field. Most are low molecular weight, for example, 2-methyl-1-[4-(methylthio)phenyl]-2-morpholinopropan-1-one (MMMP) and 2-hydroxy-2-methyl-1-phenyl-propanone (HMPP). Their structures are shown in Figure 1. The nature of a low-molecular-weight photoinitiator can be positive (good compatibility) as well as negative (foul smell and migration or evaporation). This shortcoming limits its use in some special fields, such as in food-packaging applications. The formation of organic indoor air pollutants by UV-curing chemistry was studied,[3] including the degradation processes of photoinitiators to form a number of volatile reaction products that can contribute to indoor air pollution. For example, the photoproduct of HMPP (Irgacure 1173) releases benzaldehyde, benzyl, acetone, 1-phenyl-2-methyl-1,2-propanediol, and pinacol. These compounds may have an impact on human health or olfaction. Because of environmental and legislation constraints, the use of volatile organic compounds (VOCs) in coatings is being more and more restricted. Some new photoinitiators, such as Irgacure 2959 and Irgacure 754, were produced in order to improve the

Correspondence to: J. Yang (cedc30@zsu.edu.cn).
Contract grant sponsor: National Natural Science Foundation of China; contract grant number: 20304019.

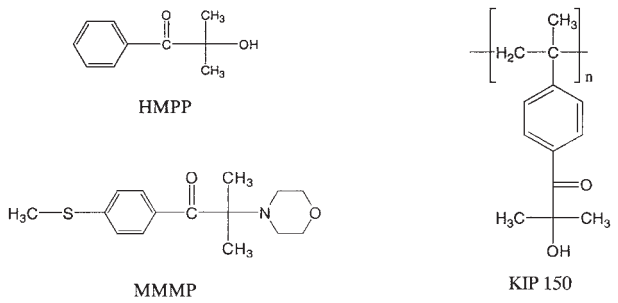

Figure 1 Structures of some commercial photoinitiators.

problem of being foul smelling without lessening photoactivity. However, the problems of emission and migration have not been overcome perfectly. Thus, macromolecules containing covalently bonded photoinitiating groups have received considerable attention.[4–6] A high-macromolecular-weight photoinitiator would be expected to have several advantages: (1) a low tendency to migrate, both in the uncured formulation and in the end product, and (2) low volatility, hence reduction of the odor problem.[7] These advantages attracted us to design and prepare new macrophotoinitiators.

Polymeric photoinitiators may be divided into three classes according to molecular weight: polymerizable photoinitiators, oligomeric photoinitiators, and macromolecular photoinitiators. Polymeric photoinitiators also can be divided into two classes according to the location of functionalities containing weaker bonds: main chain type and side group type. Polymers containing photoactive residues either in the main chain or as a side group can be prepared in two ways: (1) a photoinitiator with a suitable spacer substituent and a polymerizable group is prepared and homopolymerized or copolymerized to produce the polymeric photoinitiator; (2) the photoinitiating moiety is immobilized by a suitable chemical reaction with a reactive site on an existing polymeric backbone.[8] Until now, a variety of polymeric photoinitiators have been synthesized by these methods, mainly based on an acrylate or styrene backbone. Most of them were synthesized by the addition polymerization method. Detailed information on polymeric and polymerizable free-radical photoinitiators can be found in the review by Davidson.[9] For example, a photoinitiator named oligo{2-hydroxy-2-methyl-1-[4-(1-methylvinyl)phenyl]propanone} (KIP 150, see Fig. 1) is an oligomeric polyfunctional α-hydroxyketone characterized by high reactivity with fewer yellowing properties.[10] However, the condensation polymerization method apparently is seldom used.

For most reported polymeric photoinitiators prepared through free-radical polymerization, the photoreactive moieties exist as a pendant group for the backbone. It has been suggested that a lot of small photolysis fragments would be emitted while being irradiated under ultraviolet light, and this would not be very favorable for odorless and nonemitting UV-curable coating. In this article, a new main-chain oligomeric photoinitiator of the free-radical type was prepared by the facile method. This oligomeric photoinitiator has the photoreactive structure in the backbone, and the probability of producing volatile fragments during irradiation is considered to be reduced. On the other hand, the molecular weight of the oligomeric photoinitiator can be adjusted more easily through polycondensation than through free-radical polymerization.

EXPERIMENTAL

Materials

Diphenyl ether, provided by Peking University Zoteq Co. Ltd. (Beijing, China), was recrystallized before use. Alpha-chloroisobutyryl chloride obtained from Xinzhuang Fine Chemical Plant (Jiangning, China) and anhydrous piperazine purchased from Changzhou Shanfeng Chemical Co. Ltd. (Changzhou, China) were used without further treatment. Anhydrous aluminum chloride was chemically pure. All of the solvents utilized were dried and redistilled before use. The monomers, such as 1,6-hexanediol diacrylate (HDDA), trimethylolpropane triacrylate (TMPTA), 2-hydroxyethyl methacrylate (HEMA), were of industrial grade and provided by Beijing Eastern Acrylic Chemical Technology Co. Ltd. (Beijing, China). The photoinitiators (MMMP and HMPP) were obtained from Runtec Chemical Co. Ltd. (Changzhou, China).

Measurements

FTIR spectra were recorded on a Thermo Nicolet Nexus™ 670 FTIR ESP spectrometer (USA). The products dissolved in $CDCl_3$ at ambient temperature and the NMR spectra were obtained on a Varian Mercury 300M (Palo Alto, CA) spectrometer. The chemical shifts were reported as parts per million (ppm) down field from the tetramethylsilane. The Raman spectrum was recorded on a Renishaw RM2000 instrument with an exciting laser wavelength at 785 nm. The number-average molecular weight (M_n) and the weight-average molecular weight (M_w) of the oligomers were measured by gel permeation chromatography (GPC, Breeze GPC, Waters Corp.) using THF as the solvent. Thermogravimetric analysis (TGA; TG-209C, Netzsch Corp.) was carried out in a temperature range of room temperature to 200°C at a heating rate of 10°C/min under a nitrogen atmosphere. The UV–vis absorption spectra were measured on a Varian Cary100 spectrometer using dichloromethane and THF as solvents. A modified CDR-1 DSC (Shanghai Balance Instrument

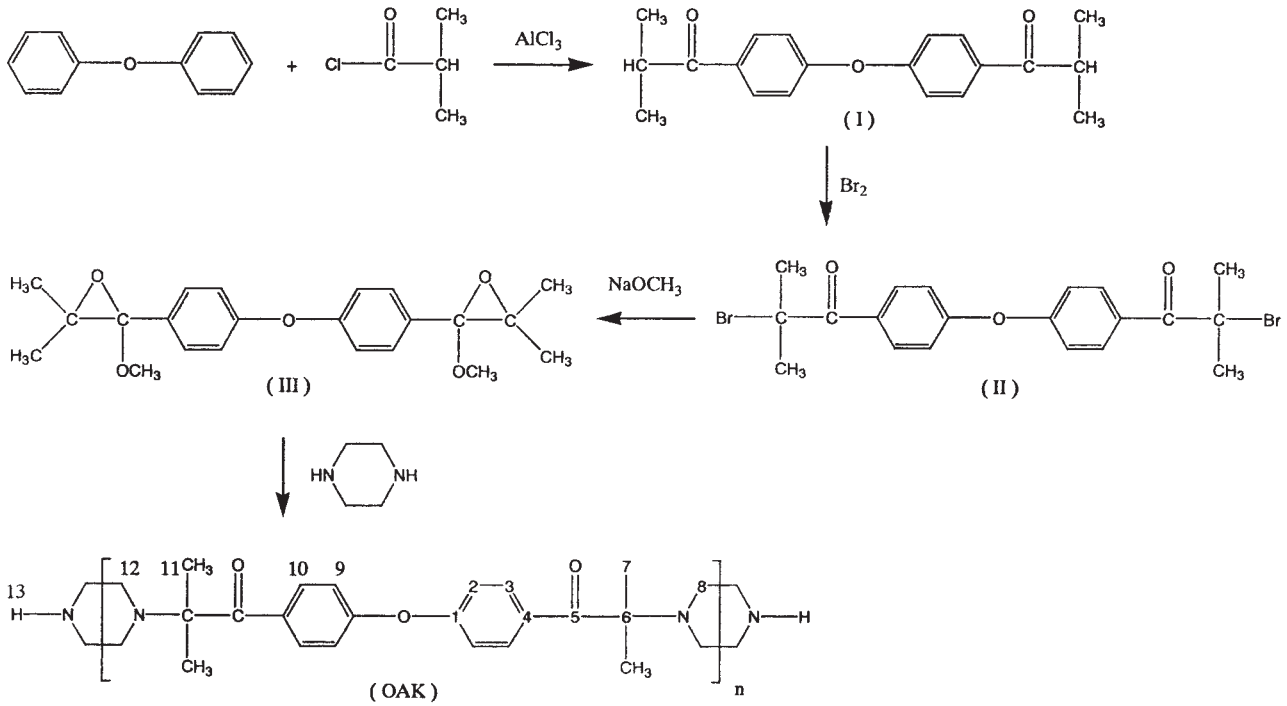

Scheme 1 Synthetic route of oligo(a-aminoketone) (OAK).

Plant) equipped with a 125-W middle pressure mercury lamp was employed to measure the exothermal rates of irradiated samples. The light intensity was measured by a UV radiometer (type UV-A, Photoeletric Instrument Factory, Beijing Normal University, Beijing, China), which was sensitive in the wavelength range of 320–400 nm. The samples containing 1–5 wt % of the initiator were sonicated for 15 min to ensure complete dissolving. A fluorescence spectrum was obtained with a FLS920 spectrometer (Edinburgh Instruments Corp.). The differential scanning calorimetry was measured using a DSC 2910 modulated instrument (TA Instruments Corp.) and heated from −30°C to 100°C at a heating rate of 10°C/min.

Synthesis of oligomeric photoinitiator

The synthesis was conducted according to the synthetic route shown in Scheme 1.

Acylation of diphenyl ether by friedel–crafts reaction

First 68 g (0.4 mol) of diphenyl ether, 113 g (0.85 mol) of aluminum chloride, and 300 mL of cyclohexane were mixed together. Then 89 g (0.84 mol) of α-chloroisobutyryl chloride was added dropwise under vigorous stirring over 1 h with the interior temperature maintained at 50°C–0°C. HCl gas was evolved. After the dropwise addition was finished, the reaction mixture was stirred at this temperature for an additional 4 h and subsequently poured into a mixture of hydrochloric acid and ice. The two phases were separated in a separating funnel. The aqueous layer was extracted with dichloromethane and combined with the organic layer collected in the first step. The combined organic phases were washed with dilute sodium bicarbonate solution, dried, and concentrated. Obtained was 110 g of bis[4-(2-methyl-propionyl)-phenyl]ether (I) with an m.p. of 40°C–41°C and a yield of 80% after being precipitated in hexane and dried a in vacuum.

FTIR (KBr pellet, cm^{-1}): 3071 (δ, aromatic C—H), 2933, 2878 (δ, CH_2, CH_3), 1680 (δ, C═O), 1588, 1499 (δ, aromatic), 1382 (δ, CH_3), 1157 (δ, C—O—C); ^{1}H-NMR (300 MHz, $CDCl_3$, δ ppm): 1.24 (d, 12H, J = 6.9 Hz, CH_3), 3.52 (m, 2H, J = 6.9 Hz, CH adjacent to carbonyl group), 7.06 (d, 4H, J = 8.7 Hz, aromatic CH close to ether oxygen atom), 7.97 (d, 4H, J = 8.7 Hz, aromatic CH close to carbonyl group); ^{13}C-NMR (300 MHz, $CDCl_3$, δ ppm): 19.6 (CH_3), 35.5 (CH), 119.0 (aromatic CH near C—O—C group), 130.8 (aromatic CH near C═O group), 132.1 (aromatic carbon adjacent to carbonyl group), 160.1 (aromatic carbon adjacent to ether oxygen atom), 203.0 (C═O).

Bromination of compound (I)

The calculated amount of fluid bromine was added dropwise at room temperature to a cyclohexane solution of compound I with stirring, and the reaction was continued for 2 h after the bromine was added. The mixture was treated with a dilute sodium hydroxide

solution, extracted with dichloromethane, and dried over anhydrous sodium sulfate. The solvent was then removed using a vacuum evaporator. The residue was poured into hexane to produce a precipitated product of bis[4-(2-bromo-2- methylpropionyl)-phenyl] ether(II) with yield of 95%, m.p. 85°C–87°C.

FTIR (KBr pellet, cm^{-1}): 3071 (ν aromatic C—H), 2976, 2932 (ν CH_2, CH_3), 1674 (ν C═O), 1584, 1499 (ν aromatic C═C), 1387 (δ CH_3), 1160 (ν C—O—C); ^{1}H-NMR (300 MHz, $CDCl_3$, δ ppm): 2.04 (s, 12H, CH_3), 7.08 (d, 4H, J = 9.0 Hz, aromatic CH close to ether oxygen atom), 8.23 (d, 4H, J = 8.7 Hz, aromatic CH close to carbonyl group); ^{13}C-NMR (300 MHz, $CDCl_3$, δ ppm): 32.1 (CH_3), 60.6 (C—Br), 118.6 (aromatic CH near C—O—C group), 130.2 (aromatic C near C═O group), 133.0 (aromatic CH near C═O group) 159.6 (aromatic C near O atom), 195.1 (C═O); Elem. Anal Calcd for $C_{20}H_{20}Br_2O_3$: C, 51.31%; H, 4.31%. Found: C, 51.37%; H, 4.26%.

Epoxidation of compound (II)

Twenty-one grams (0.045 mol) of compound II was heated to 80°C–90°C, and 200 mL of a solution of sodium methoxide (approximately 1.2 mol/L) was added dropwise at reflux temperature. The reaction lasted for 7 h at 80°C. Methanol was then distilled off, and ethyl ether was poured into the residue. The filtrate was washed with water, dried, and concentrated. Obtained was 15 g of bis[4-(2-methoxy- 3,3-dimethyl-oxiranyl)-phenyl] ether (III) with a yield of more than 90%.

FTIR (KBr pellet, cm^{-1}): 3070, 3040 (ν aromatic C—H), 2937, 2831 (ν, CH_2, CH_3), 1600, 1460 (ν aromatic C═C), 1440, 1380 (δ CH_3), 1165 (ν C—O—C), 897(ν epoxy group); ^{1}H-NMR (300 MHz, $CDCl_3$, δ ppm): 1.05 (s, 6H, CH_3), 1.55 (s, 6H, CH_3), 3.24 (s, 6H, OCH_3), 7.04 (d, 4H, J = 8.7 Hz, aromatic CH close to ether oxygen atom), 7.44 (d, 4H, J = 8.7 Hz, aromatic CH close to OCH_3 group); FAB-MS: calcd M = 370 for $C_{22}H_{26}O_5$ and found $(M+1)^+$ = 371.

Preparation of oligo(α-aminoketones) (oak) from epoxide (III)

Epoxide (III) was treated with a stoichiometric amount of piperazine in an autoclave and reacted for 10–20 h at 200°C. The product was dissolved in dichloromethane, and the concentrated solution was poured into ethyl ether. The precipitate was separated out and dried in a vacuum oven. The yield was about 75%–90%.

FTIR (KBr pellet, cm^{-1}): 3490–3400 (ν N—H), 3070 (ν aromatic C—H), 2940, 2820 (ν CH_2, CH_3), 1676 (ν C═O), 1590 (ν aromatic C═C), 1490 (ν aromatic C—H), 1460, 1380 (δ CH_3), 1151 (ν C—O—C); ^{1}H-NMR and ^{13}C-NMR are shown in Figures 2 and 3. The UV spectrum (CH_2Cl_2) is shown in Figure 4.

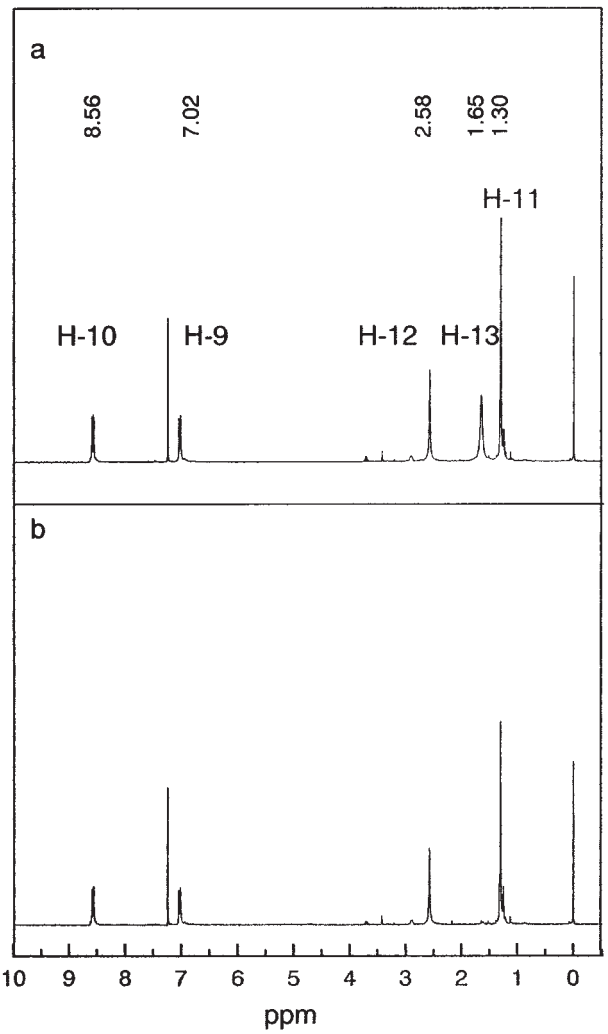

Figure 2 ^{1}H-NMR spectra of OAK in $CDCl_3$: (a) common spectrum, (b) D_2O exchange spectrum.

RESULTS AND DISCUSSION

Investigation of spectra

NMR spectroscopy

Figures 2(a) and 3(a) show the ^{1}H- and ^{13}C-NMR spectra of OAK in $CDCl_3$. The assignment of the chemical shifts is marked in the two spectra and Scheme 1. The D_2O exchange investigation [Fig. 2(b)] revealed the assignment of N—H (δ 1.65 ppm). This broad peak resulted from the effect of the quadrupole moment relaxation of N atom. Figure 3(a) shows that the two peaks in 131.0–133.0 ppm are very close, they were able to be identified by DEPT-135 measurement [Fig. 3(b)]. The sharp resonance signal of a positive phase at 132.3 ppm could be assigned to C-3, and the disappearance of the signal revealed the position of the

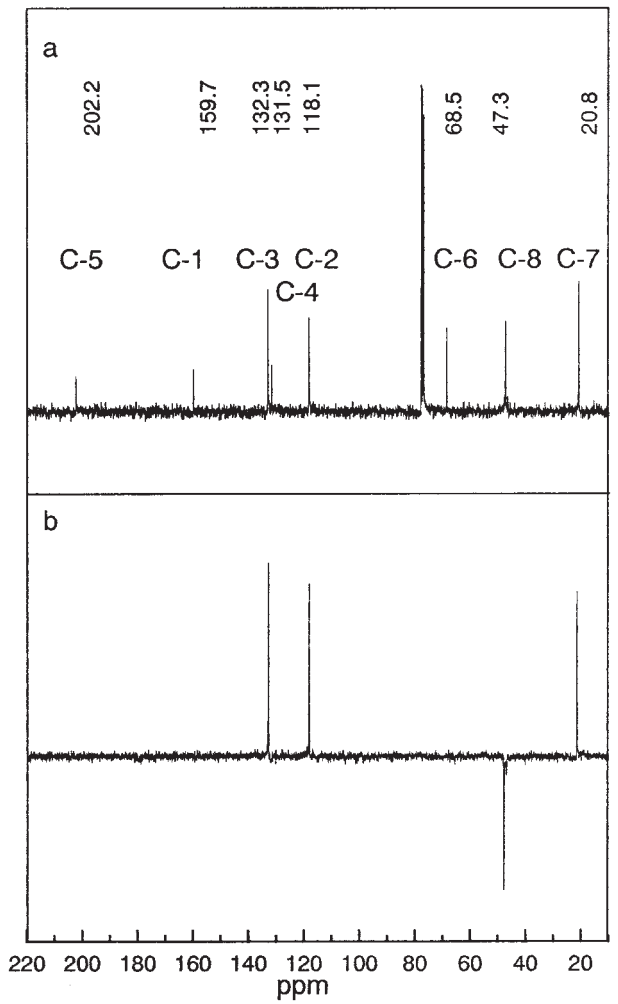

Figure 3 ^{13}C-NMR spectra of OAK in $CDCl_3$: (a) common spectrum, (b) DEPT spectrum ($\theta = 135°$).

quaternary carbon in benzene ring (C-4, 131.5 ppm). The CH_2 in piperazine ring (47.3 ppm) appeared as a negative phase in this DEPT spectrum.

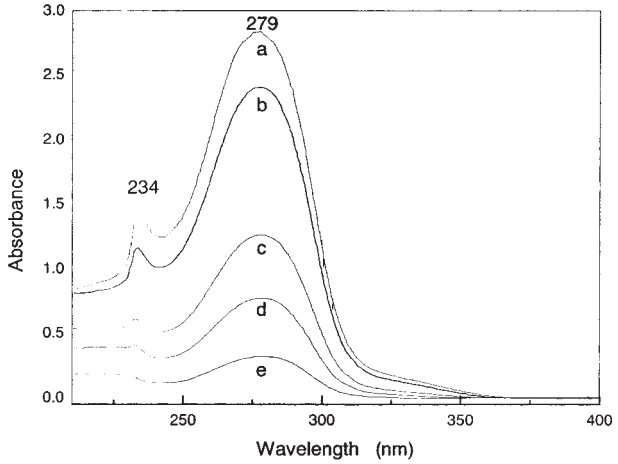

Figure 4 UV–vis spectra of OAK in CH_2Cl_2 (M_n = 2691): (a) 5.8×10^{-2} g/L, (b) 4.4×10^{-2} g/L, (c) 2.2×10^{-2} g/L, (d) 1.5×10^{-2} g/L, (e) 6.0×10^{-3} g/L.

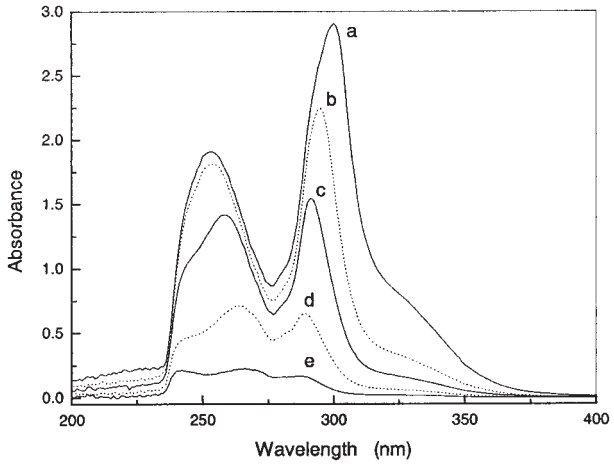

Figure 5 UV–vis spectra of macrophotoinitiator OAK in THF (M_n = 2691): (a) 2.3×10^{-1} g/L, (b) 9.4×10^{-2} g/L, (c) 4.7×10^{-2} g/L, (d) 1.9×10^{-2} g/L, (e) 4.7×10^{-3} g/L.

UV–vis spectroscopy

Figure 4 shows the absorption peaks of the obtained oligomeric photoinitiator containing a *tert*-amine structure are at 234 and 279 nm in CH_2Cl_2, with corresponding molar extinction coefficients (ε_{max}) of 7.1 $\times 10^4$ L mol^{-1} cm^{-1} (234 nm) and 1.5 $\times 10^5$ L mol^{-1} cm^{-1} (279 nm), respectively. OAK concentration seemed to have had no effect on the absorption wavelength in CH_2Cl_2. However, the absorption in THF was greatly different from that in dichloromethane, as shown in Figures 5 and 6. For the sample in dichloromethane, the oligomer chains may have been entangled, folded, and/or stuck together through intermolecular hydrogen bonding of end piperazine, which led to a broad absorption band without fine structure because of the mutual interaction of the absorption

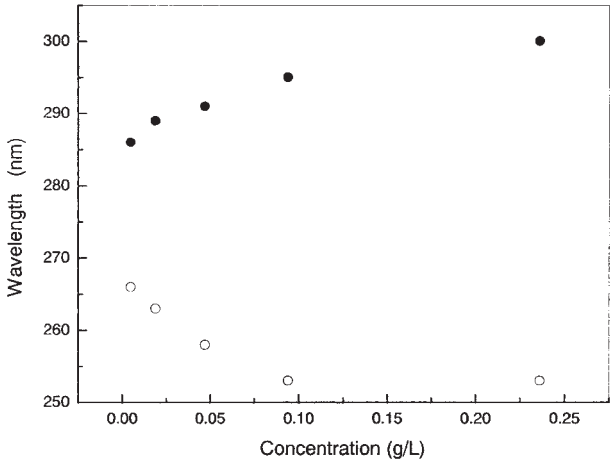

Figure 6 Dependence of the positions of the absorption peaks versus OAK concentration in THF: ● for high wavelength absorption, ˆ for low wavelength absorption.

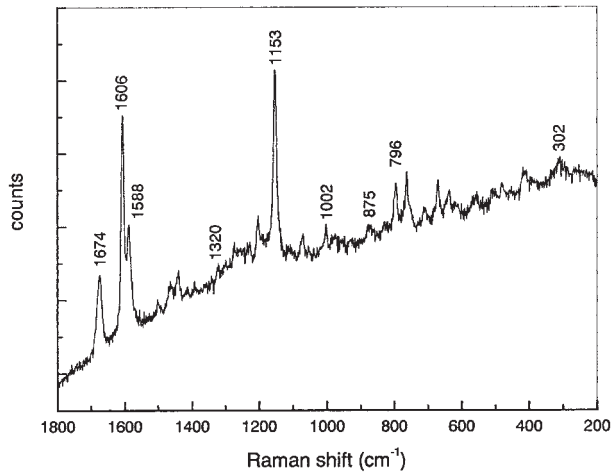

Figure 7 Raman spectrum of OAK (M_n = 2691) with exciting laser at a wavelength of 785 nm.

moieties. Although THF was used as the solvent, the forming of a hydrogen bond between THF and end piperazine was helpful for the separation of the entangled and/or stacked oligomer chains. Thus, the sample inclined toward producing a separated absorption band with less interchain interaction. Of course, additional evidence is needed for this explanation.

Raman spectroscopy

The baseline of the Raman spectrum was slanted because of the fluorescence (Fig. 7). The strong scattering peak at 1674 cm^{-1} could be assigned to a carbonyl stretching vibration mode. The sharp peaks at 1606 and 1588 cm^{-1} indicate a benzene ring.[11] Based on the literature,[12,13] the stokes shift for the C—N bond may be found at 1320 cm^{-1}. The other Raman shifts may be attributed as: 1153 cm^{-1} (C—H distortion of aromatic ring), 796 cm^{-1} (γ C—H), 1002 cm^{-1} (breathing vibration of benzene ring), 875 cm^{-1} (ring breathing band of piperazine), and 302 cm^{-1} (long-distance vibration of polymer chain).

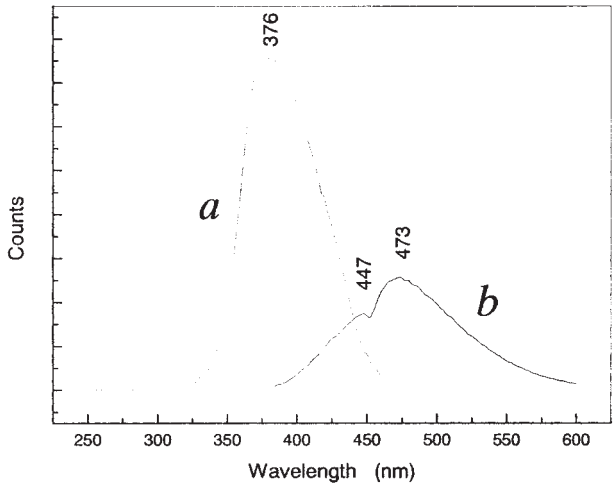

Figure 8 Fluorescence spectra of OAK (M_n = 2691) in CH_2Cl_2 (c = 0.88 g/L): (a) excitation spectrum, (b) emission spectrum.

TABLE I
GPC Analyses of OAK Series

Sample	Epoxide (mol)	Piperazine (mol)	M_n (D)	M_w (D)	Polydispersity
OAK-1	0.02	0.033	2030	2392	1.17
OAK-2	0.02	0.029	2581	3426	1.32
OAK-3	0.02	0.027	2691	3544	1.31
OAK-4	0.02	0.023	3011	4558	1.51
OAK-5	0.02	0.022	3144	4935	1.56

Fluorescence spectroscopy

The emission spectrum is usually utilized to investigate the excited state of a photoactive molecule. The steady-state fluorescence spectra of OAK in CH_2Cl_2 are shown in Figure 8. A broad fluorescence signal was obtained without fine structure information. The oligomer had a maximum excitation wavelength (λ_{ex}) at 376 nm and maximum emission (λ_{em}) at 473 nm.

Molecular weight

To investigate the influence of molecular weight on initiation efficiency, five OAK samples with different molecular weights were prepared according to the feed ratios listed in Table I. The corresponding investigation, to be completed, will be included in a future submission. The measured molecular weight and polydispersity of the oligomers were obtained through the GPC curves displayed in Figure 9. An oligomeric photoinitiator with a number-average mo-

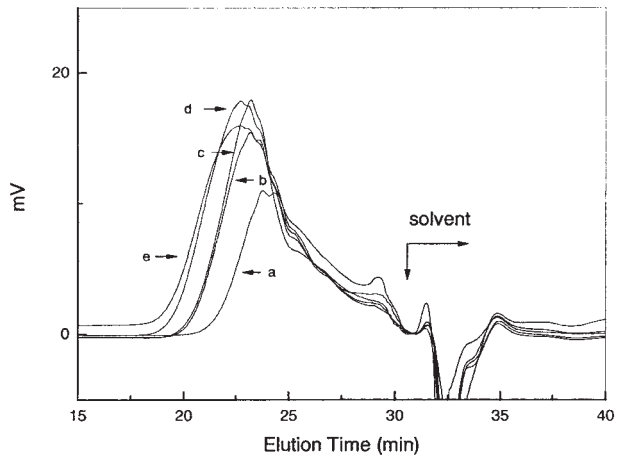

Figure 9 GPC traces of OAK series in THF: (a) OAK-1, (b) OAK-2, (c) OAK-3, (d) OAK-4, (e) OAK-5.

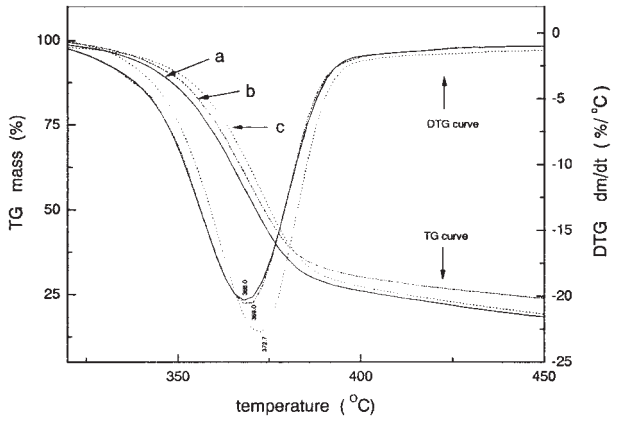

Figure 10 T_g and DT_g curves of OAK (heating rate: 10°C/min): (a) M_n = 2581, (b) M_n = 2691, (c) M_n = 3144.

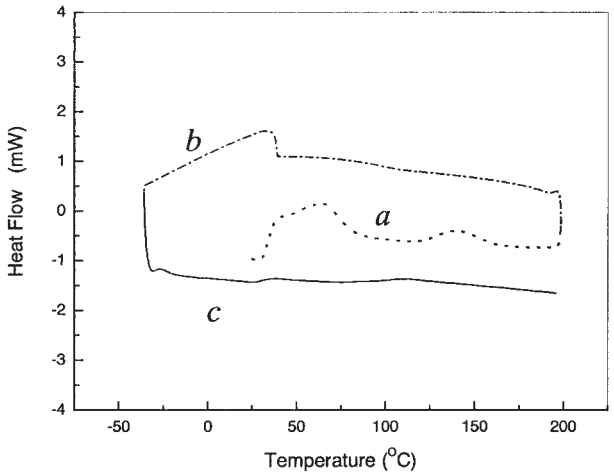

Figure 11 DSC cures of OAK: (a) first scanning, (b) cooling, (c) second scanning (heating rate: 10°C/min).

lecular weight ranging from 2000 to 4000 could be obtained by adjusting the molar ratio of epoxide/piperazine. This result supports the practice of using the synthetic method. In addition, most of the polydispersity indices were below 1.6, indicating a narrow molecular-weight distribution, which is not surprising considering the low degree of polycondensation.

Thermal analysis

The T_g curves and differential thermogravimetric (DT_g) curves for OAK are shown in Figure 10. Perfect thermal stability of OAK was observed below 250°C, as indicated by the T_g curve. The weight loss, which began at 287°C and was completed at 412°C, with a mass loss of about 80%, was considered mainly a result of the thermal decomposition. The maximum weight-loss temperature was 367°C, and this temperature increased slightly with the molecular weight of OAK. The excellent thermal stability of OAK means less volatility, which is beneficial to environmental protection and which has an aesthetic olfactory effect while used as a photoinitiator in UV-curable coatings for the decoration of the packaging of goods.

The DSC curve (Fig. 11) shows that neither an endothermic nor an intense exothermic process occurred during the second heating process. No peak in the temperature range of 30°C–200°C could be detected, suggesting that the oligomer was a noncrystalline material.

Photoinitiation efficiency

It is well established that the photodecomposition of HMPP and MMMP follows the Norrish I cleavage mechanism.[14] In this investigation, photo-DSC was employed to evaluate the photoinitiating efficiency of OAK. During the comparative photo-DSC experiment, which was based on a formulation of HDDA, OAK was shown to perform competitively with low-molecular-weight photoinitiators (as shown in Fig. 12). The induction period for HMPP is shorter than that for OAK and MMMP, but the ultimate conversion is almost the same. In the oligomer structure, the photoactive oligomer had a weak α C—C bond, with dissociation energy lower than the excitation energy of its reactive excited state. α-Cleavage occurred when the sample was exposed to UV light. The proposed photodecomposition process is shown in Scheme 2. Because the oligomer has two weak C—C bonds within a repeat unit, perhaps biradical intermediates appear in the photodecomposition outgrowth. This can increase the initiating efficiency or the probability of a fragment being bonded to the backbone of the formed polymer chain. As it is hard for a photoinitiator of the usual formulation to reach complete photoscission,

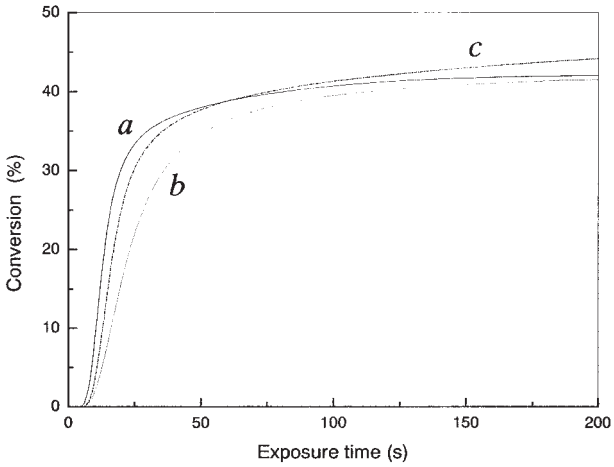

Figure 12 Conversion curves for HDDA (at room temperature in nitrogen atmosphere and light intensity of 4 mW/cm^2) initiated by: (a) 3.6 wt % HMPP (D 1173), (b) 4.0 wt % OAK-1 (M_n = 2030), (c) 5.8 wt % MMMP (Ir 907).

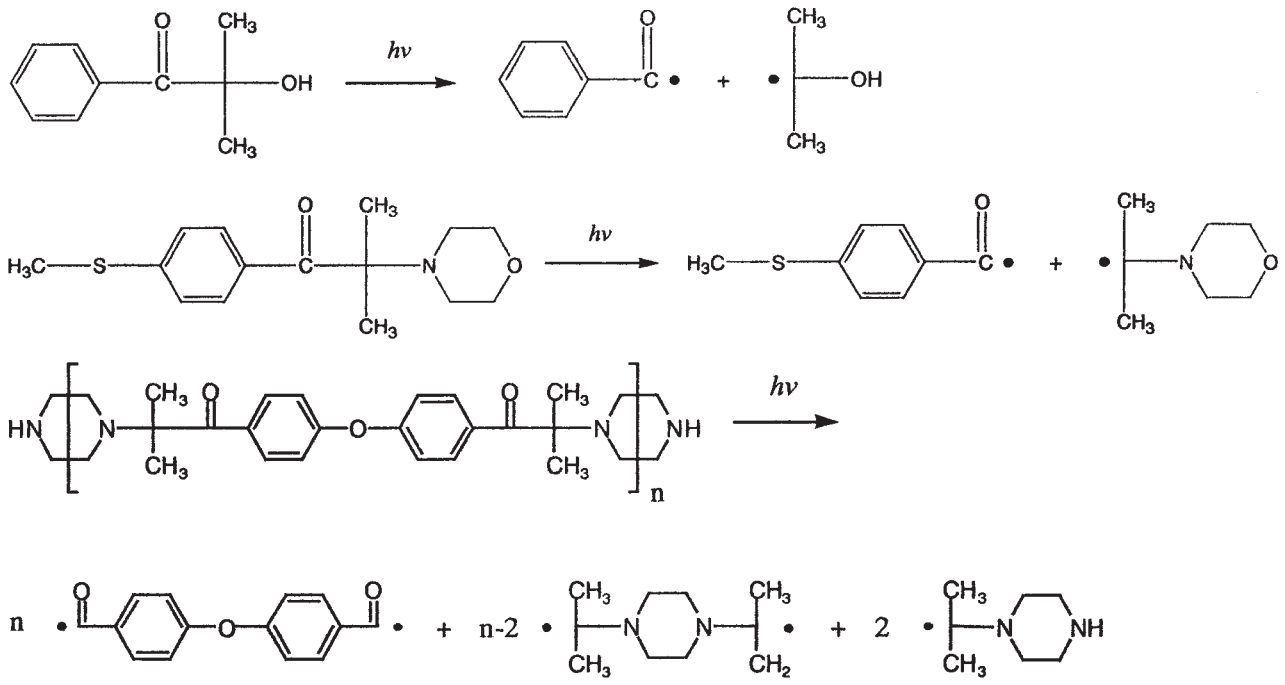

Scheme 2 Proposed mechanism for photolysis of the oligomeric photoinitiator (OAK).

the oligomeric photoinitiator that is left, including the residual photoactive moieties attached to the polymer chain produced, will keep its initial oligomeric state, thus obtaining the properties of low migration and low volatility. Even for the photolysed oligomeric molecule, the small molecular byproducts of the free-radical fragments exhibit high enough molecular weight to prevent volatilization.

CONCLUSIONS

An oligomeric photoinitiator with a molecular weight (M_n) of 2000–4000 was synthesized and fully characterized. The yield (60%–80% overall) was high enough to meet practical requirements. Preliminary photo-DSC investigation suggested the possible application of this oligomeric photoinitiator for UV-curable coating. Its thermal stability enabled it to avoid the problem of VOCs and to increase its aesthetic olfactory effect when used in UV-curable coatings.

References

1. Fouassier, J. P.; Ruhlmann, D.; Graff, B.; Wieder, F. Prog Org Coatings 1995, 25, 169; Fouassier, J. P.; Ruhlmann, D.; Graff, B.; Morlet-Savary F.; Wieder F. Prog Org Coatings 1995, 25, 235.
2. Dietliker, K. In Chemistry & Technology of UV & EB Formulation for Coating, Inks & Paints; Oldring PKT, Ed.; SITA Technology: London, 1991; Vol. 3, Chapter 1.
3. Salthammer, T.; Bednarek, M.; Fuhrmann, F.; Funaki, R.; Tanabe, S.-I. J Photochem Photobiol, A: Chem 2002, 152, 1; Salthammer, T.; Schwarz, A.; Fuhrmann, F. Atmos Enviro 1999, 33, 75.
4. U.S. Pat. 4,922,004 (1990).
5. WO2004009651 (2004).
6. Seok, J. W.; Ryu, H. S.; Seo, H. J.; Kim, W. S.; Lee, D. H.; Min, K. E.; Seo, K. H.; Kang, I. K.; Park, L. S. Opt Mater 2003, 21, 633.
7. Chen, Y. L.; Zeng, Z. H., Yang; J. W. Radiation Curable Materials and Application; Chemical Engineering Press of China: Beijing, 2003; Chapter 4.
8. Gruber, H. F. Prog Polym Sci 1992, 17, 953.
9. Davidson, R. S. J Photochem Photobiol A: Chem 1992, 69, 263.
10. Segurola, J.; Allen, N. S.; Edge, M.; McMahon, A.; Wilson, S. Polym Degrad Stab 1999, 64, 39.
11. Ke, Y. K.; Dong, H. R. Handbook of Analytical Chemistry, Vol. 3: Spectroscopic Analysis; Chemical Industry Publisher: Beijing, 1977; p 1151.
12. Chen, J.; Hu, J. M.; Xu, Z. S.; Sheng, R. S. Applied Spectroscopy 1993, 47, 292.
13. Chen, J.; Hu, J.; Xu, Z.; Sheng, R. Spectrochim Acta, Part A 1994, 50, 929.
14. Jockusch, S.; Landis, M. S.; Freiermuth, B.; Turro, N. J. Macromolecules 2001, 34, 1619.